SLAC NATIONAL ACCELERATOR LABORATORY

COMPASS Accelerator Design Technical Overview

Emilio Nanni, Valery Dolgashev, Sami Tantawi, Jeff Neilson

ABSTRACT

This report is a survey of technical options for generating a MeV-class accelerator for space based science applications. The survey was performed focusing on the primary technical requirements of the accelerator in the context of a satellite environment with its unique challenges of limited electrical power (PE), thermal isolation, dimensions, payload requirement and electrical isolation.

SLAC-R-1058 January 28, 2016

This material is based upon work supported by the U.S. Department of Energy, Office of Science, Office of Basic Energy Sciences, under Contract No. DE-AC02-76SF00515 and NSF.

Table of Contents

Introduction

We have performed a survey of the technical options for generating the electron beam described in the COMPASS proposal. The survey was performed focusing on the primary technical requirements of the accelerator in the context of a satellite environment with its unique challenges of limited electrical power (P_E), thermal isolation, dimensions, payload requirement and electrical isolation. This experimental apparatus is envisioned for deployment with a MIDEX class satellite.[1] The general range of parameters for this class of satellite is given in Table 1. We focused our efforts on four technical approaches to the accelerator which we found to be credible with varying degrees of technical risk: (1) normal-conducting linear accelerator (LINAC) powered by a magnetron, (2) normal-conducting LINAC powered by a solid-state power amplifier (SSPA), (3) superconducting LINAC powered by a SSPA and (4) normal-conducting microtron (multi-pass cavity) accelerator powered by a SSPA.

Table 1: MIDEX Class Satellite Parameters

Electrical Power (P_E)	250 W
Dimensions – External Payload	2 m Diameter, 2 m Length
Temperature Range	-20 C – 70 C
Payload	750 kg

The dominant consideration in designing the accelerator is the available electrical power (P_E) on board the satellite, Table 1. An accelerator has a diverse set of components which operate with electrical power requirements that we place in three categories: CW (P_E^{CW}), transient (P_E^{T}) and instantaneous (P_E^{I}). Stable operation is achieved when electrical power available on the satellite can meet the average power requirements of all components or $P_E = \langle P_E^{CW} \rangle + \langle P_E^{T} \rangle + \langle P_E^{I} \rangle$. Components in the CW power category, such as filament heaters, heat exchangers and vacuum pumps, require time to reach steady-state operation, need power continuously during the operation of the accelerator and are the first systems that are turned on. Components in the transient power category, such as magnets and diagnostics, can be turned on and off more rapidly than CW components, but should remain while generating the electron beam. In the instantaneous power category, such as the RF source and electron beam, draw power only when generating the electron beam. Due to these electrical power requirements, the accelerator would operate under a unique electrical power load sequence that to meet the available electrical power the satellite. A schematic of the accelerator electrical power load sequence is shown in Figure 1.

The electrical power load sequence of the accelerator can be described quantitatively by two duty cycle values: D_{RF} for the electron-beam pulse and D_{ME} the measurement sequence, with the cycles shown in Figure 1 and labeled as 'Beam Emission Cycle' and 'Measurement Cycle', respectively. As the RF source technology and accelerator design are varied a wide range of parameters are explored for D_{RF} and D_{ME} to optimize performance.

We define as the figure of merit for each technology the electron beam power averaged over the measurement cycle (P_b^m) exiting the satellite. P_b^m is a direct measure of the total signal power available for earth-based detection. With an increase in P_b^m the signal to noise ratio improves. This differs from the electron beam power averaged over the beam emission cycle (P_b^{RF}) which is the signal power required for earth-based detection. Any realistic accelerator must achieve the P_b^{RF} required for detection, and the technical approach with the largest P_b^m for a given P_b^{RF} will produce the largest detected signal.

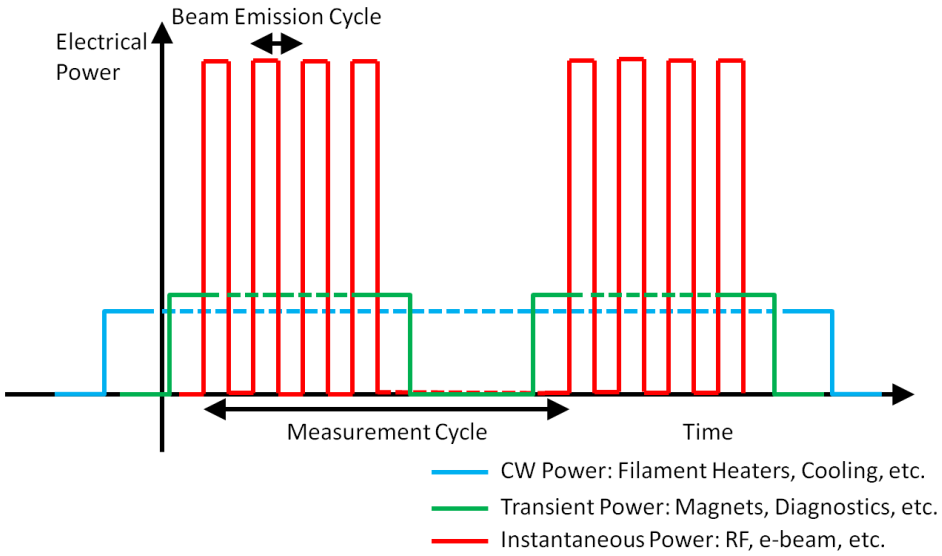

Figure 1: Schematic for accelerator electrical power load sequence. Accelerator components are organized into three categories: CW, transient and instantaneous. The electrical power drawn by each category is plotted as a function of time.

COMPASS Performance Specifications

For this report we will define a nominal set of parameters, listed in Table 2, for the operation of the accelerator at which we compare the various potential design approach approaches. The worksheets which calculate the performance parameters of the four accelerator designs use these inputs from Table 2 as variables and they can be adjusted as the electron beam requirements change with mission scope or detector technology. The explored parameter space by these four accelerator designs is listed in Table 3. The operation points for the four designs are shown as a function of peak current with RF duty cycle in Figure 2.

Table 2: Target LINAC Performance

Energy	1 MeV
LINAC Length	1 m
Electron Beam Power Averaged Over Beam Emission Cycle (P_b^{RF})	100 W

Table 3: Explored Parameter Space for Achieving P_b^{RF} =100 W

	Minimum Duty Cycle	Maximum Duty Cycle
RF Duty Cycle (D_{RF})	0.1 %	100%
Peak Current	0.1 A	100 μA
Peak Electron Beam Power	100 kW	100 W
RF Frequency	1 – 10 GHz	

The focus of this report is to provide an analysis of the required equipment and a direct comparison between the P_b^m of the four designs. We do not compare the achievable electron beam quality in terms of

source size, divergence and energy spread which require more detailed studies. The electron beam quality produced by the four designs could vary significantly because the peak electron beam current in the accelerator varies widely over this parameter space, see Figure 2. The accelerator design becomes increasingly challenging with higher peak current, which is one advantage of operating with longer RF duty cycles. Before specifying the required electron beam quality more information is needed on the earth-based detector.

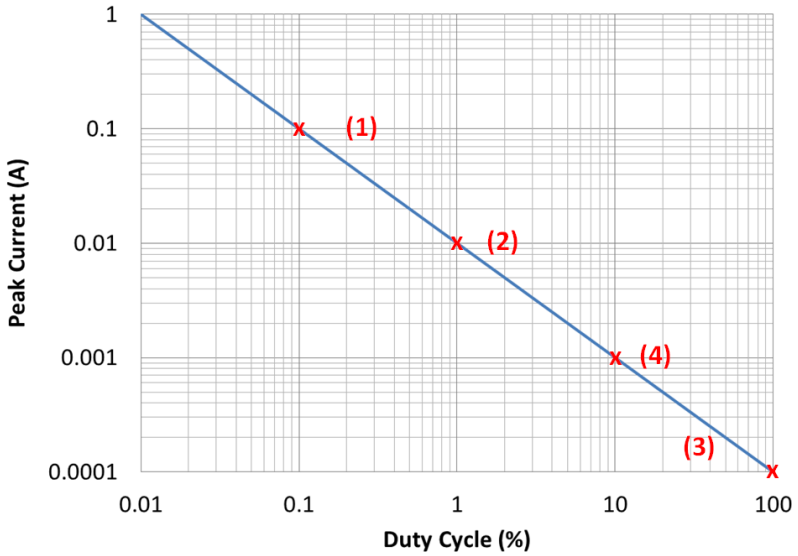

Figure 2: The peak current as a function of RF duty cycle for P_b^{RF} = 100 W . The peak power can be calculated by multiplying the peak current by the beam voltage (1 MV). Design cases detailed in the report are marked with 'x' and labeled in red.

RF Cavities

The overall performance of the accelerator is fundamentally determined by the RF properties of the electromagnetic cavities which interact with the electron beam. Therefore, we begin by reviewing the design of the cavities used in this study in the following subsections. The cavities must be powered by RF sources. In turn, the performance or availability of the RF sources places constraints on the cavity design. For reference the performance parameters of the various RF sources which are used to power these cavities are listed in Appendix A: RF Source Technology. Commercial sources were chosen to provide a baseline realistic assessment of present technological capabilities with high reliability.

Normal-Conducting Linear Accelerator

Normal-conducting cavities used to make standing-wave accelerating structures can provide a very large shunt-impedance (a measure of electrical efficiency) for accelerating electrons. These structures can be operated over a wide range of duty cycles which allows them to be used for both design (1) powered by a magnetron (Appendix A.a.i) at 0.1% duty cycle and design (2) powered by an SSPA (Appendix A.b) with up to a 10% duty cycle. The achievable shunt-impedance over a wide frequency range (1-12 GHz) is approximately 130-150 MΩ/m[2,3,4]. Therefore, operating at higher frequencies is preferable to limit the

physical size of the accelerator (the radius scales linearly with frequency). However, RF sources become more costly and difficult to fabricate with increasing frequency. For this reason we select 9.3 GHz, which is the highest frequency where vacuum electron devices and SSPAs are both commercially available with sufficient power. For the target LINAC performance listed in Table 2 we plot, in Figure 3, the required peak and average RF power as a function of the RF duty cycle.

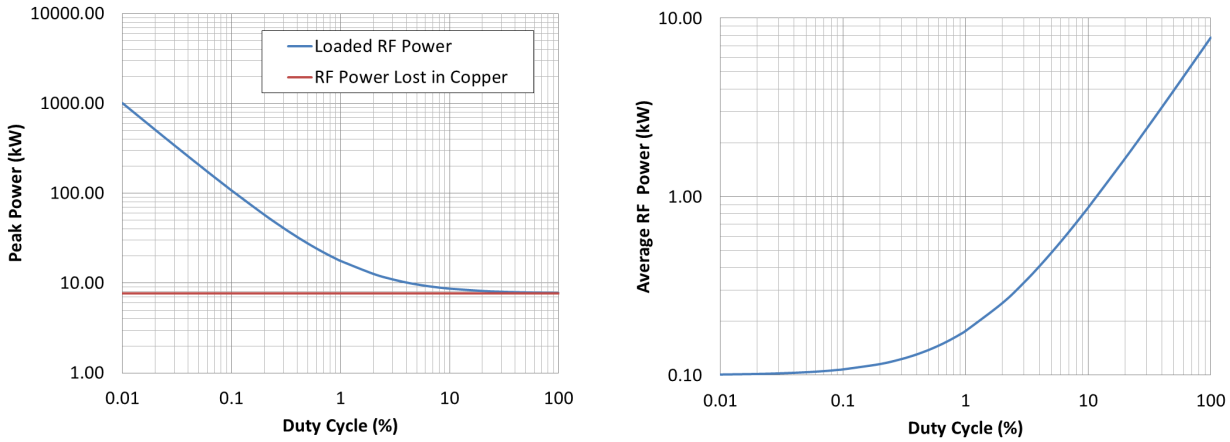

(a) (b)

Figure 3: (a) Peak power required as a function of duty cycle for a 100 W (P_b^{RF}) electron beam accelerated to 1 MeV in 1 m with a 130 MΩ shunt impedance. The red line indicates the power needed to reach this accelerating gradient, which is absorbed by the copper. The blue line includes power lost in the copper and power to accelerate the electron beam. (b) The average RF power provided to the LINAC over D_{RF}.

From these figures we can infer two things. First, at very low RF duty cycles (<0.1%) we require a vacuum electron device due to the very high peak power. Second, the average power required to power the LINAC increases rapidly above 1% due to power loss in the copper walls of the LINAC. Therefore, operating with duty cycles of a few percent or less is advantageous for the electrical power (P_E^I). required by the accelerator. Duty cycles below 0.1% do not provide any additional advantage to the average power required, because almost all of the energy is used to accelerate the electron beam.

Superconducting Linear Accelerator

Superconducting cavities used in standing wave LINACs can provide the highest shunt impedance available, with a demonstrated shunt impedance of 10^7 MΩ/m.[5] Typically, these cavities are immersed in liquid helium to maintain a stable temperature and superconductivity. The superconducting cavities have losses at RF frequencies[6], but these losses are very small compared to copper. However, even the very small amount of RF power deposited into the structure must be removed to maintain the temperature of the LINAC at 4.2 K. In a large earth-based cryo-module this thermal energy can be removed from the cryostat at a rate of 240 W/W. Data from cryogenic cooling systems from previous space bound missions demonstrated performance of approximately 1025 W/W[7,8,9] which is significantly worse due to the reliance on radiative cooling for the spacecraft as opposed to using a large heat sink such as a water bath. The electrical power (P_E^{CW}) required to cool the LINAC will be a constant load on the satellite's power supply and is the primary factor in limiting the measurement power P_b^m. The losses in the cavity increase

with frequency; therefore we select 1.3 GHz as the operating frequency for the cavity to limit losses while maintaining an acceptable dimension for the cavity.

Normal-Conducting Microtron

A microtron is an electron accelerator which uses a single RF cavity to accelerate the electron beam by sending it on a spiral path in a fixed magnetic field and passing through the cavity many times (~20). In a traditional microtron the energy gain of the electron is equivalent to the rest energy of the electron per pass to maintain synchronism. This requires a large electric field in the cavity which cannot be produced with the available electrical power (P_E) on the satellite. We designed an isochronous microtron were the electron orbit time is held constant as it accelerates due to a radially increasing magnetic field (similar to an isochronous cyclotron). This allows for a compact design with lower power requirements and a permanent magnet[10]. With only one cavity, shown in Figure 4(a) and the desire to use a low magnetic field we select 1.3 GHz for operation. For comparison with LINAC cavities we define a shunt impedance for the microtron as of the energy gain per pass divide by the cavity length. The microtron cavity has a shunt impedance of 20 MΩ/m which is a significantly lower shunt impedance than a LINAC cavity due to

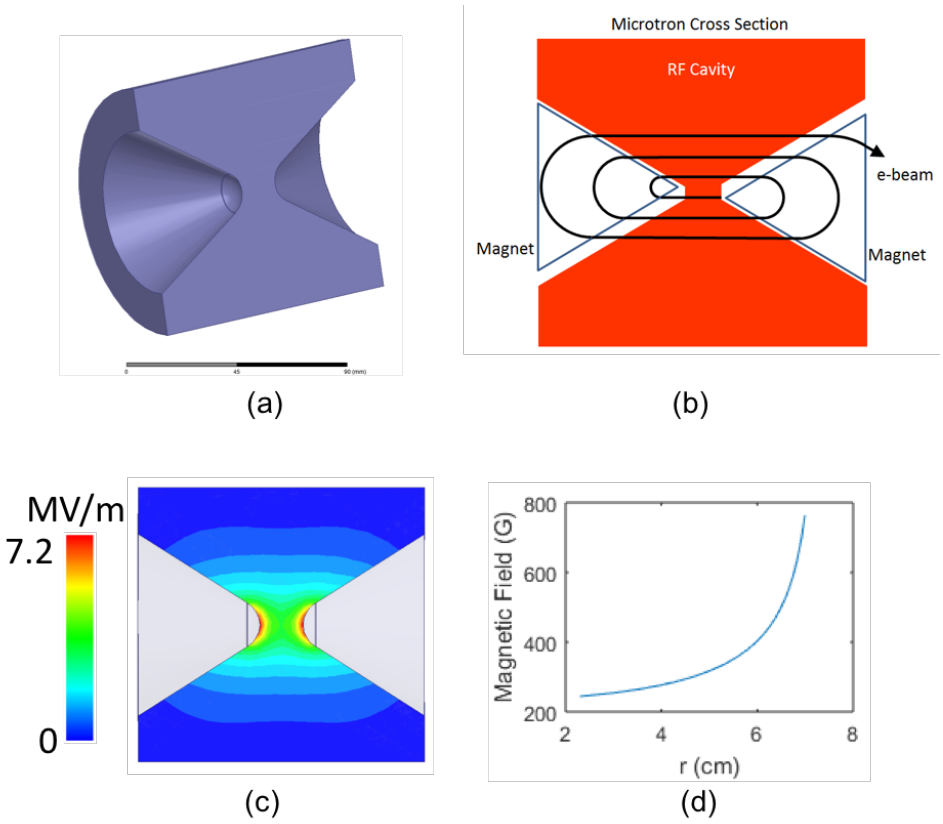

Figure 4 (a) The vacuum space inside one half of the RF cavity. (b) Schematic of the cross section of the microtron RF cavity and bending magnets. (c) Magnitude of the electric field in the RF Cavity along the cross section shown in (b). (d) Magnetic field required as a function of beam radius.

geometrical constraints. However, by using multiple passes the efficiency of the device is increased. Similar to the normal-conducting LINACs a duty cycle of ~1 % is advantageous in lowering the average power required. However, the microtron will be more sensitive to the beam current that a LINAC and for this reason we list parameters at 10% duty cycle. Figure 4(b) shows a cross sectional schematic of the microtron with the electron orbit shown as it is accelerated multiple times in the same RF cavity. Figure 4(c) is the magnitude of the electric field in the same plane as the schematic for half of the RF cavity. Figure 4(d) is the magnetic field required to maintain synchronism with the RF field as a function of the electron beam radius. This magnetic field can be produced by permanent magnets with no electrical power needed.

Comparison of Accelerator Designs

Summary of Accelerator Design Performance

In this sub-section we present a summary of the performance parameters for the four designs which were investigated assuming the design constraints given in Table 1 and Table 2. The subsequent sub-sections will discuss some of the specifics including major advantages, concerns for the different approaches and potential design improvements (both to the accelerator and auxiliary systems which were limited to current off the shelf (COTS) equipment). In Table 4 we list the performance for each design. Overall we note that all four approaches can deliver similar P_b^m. This indicates that all of these technologies are competitive from a performance perspective. However, the technical complexity and risk of the various approaches does have some significant variation. We also note that there are parameters such as available electrical power (P_E) and output electron beam energy which could quickly eliminate certain approaches from consideration. These issues are discussed in the following subsections.

Table 4: Summary of Accelerator Design Performance Consuming 250 W Electrical Power

Accelerator Parameters: 1 MeV, 1 m , P_b^{RF} =100 W

Design	LINAC Weight (kg)	Total Weight (kg)	Freq. (GHz)	D_{RF} (%)	D_{ME} (%)	*Average Beam Power* - P_b^m (W)
(1) LINAC – Magnetron	14	150	9.3	0.10	46	**46**
(2) LINAC – SSPA	14	94	9.3	1	27	**27**
(3) CW Super-conducting LINAC	13	32	1.3	100	49	**49**
(4) Microtron	10	31	1.3	10	48	**48**

Design (1): Normal-Conducting LINAC Powered by Magnetron

Advantages:

The high peak power of the magnetron makes this LINAC very efficient for the average P_E^I and P_E. Scales well to higher energy electron beam.

Disadvantages:

The CW power (see Figure 1) required by the magnetron is very high due to the power required to run the thermionic cathode (See Appendix A.a.i). Operating this design with a long-term electrical power supply of less than 100 W seems unlikely and below 75 W is impossible. The high-voltage at which the magnetron operates adds significant complexity and weight to the accelerator design. A heavy and large high-voltage modulator to power the magnetron is required (See Appendix B). If the beam power required is increased above P_b^{RF}=100 W the magnetron will need to be replaced with a more powerful version (See Appendix A.a.ii).

Potential Improvements:

A RF source with a longer pulse and a lower repetition rate format but the same duty cycle (currently 3.5 μs, 285 Hz) will improve electrical efficiency of the modulator (15% improvement) due to reduced losses in the transient portion of the high-voltage pulse.

A custom designed modulator providing the minimum power necessary could provide significant weight reductions (10s kg).

Design (2): Normal-Conducting LINAC Powered by SSPA

Advantages:

Solid-state RF sources do not require a high-voltage modulator. SSPA requires power only when the LINAC is on, unlike RF sources with thermionic emitters. Good for beams with high P_b^{RF}, because it can operate with a longer duty cycle (D_{RF} which reduces the number of SSPA to power the LINAC.

The bandwidth of the solid-state amplifier would allow changes in LINAC frequency due to temperature shifts to be compensated electronically by tuning of drive frequency.

The accelerator is more fault tolerant due the presence of multiple RF sources and distributed coupling of RF power into the accelerator.

Disadvantages:

The lower efficiency of solid-state sources and the need for a complex array of powering elements for the LINAC. Above 1 MeV output energy the LINAC length needs to be increased to maintain reasonable peak power requirements, but this could be done with bending magnets in a compact serpentine geometry, see Figure 5.

Potential Improvements:

A 180^o bend using a dipole magnet could be introduced to double the length of the accelerator in a compact geometry, see Figure 5. This reduces the RF power required by a factor of two. (The peak power required is ¼ but we need to fill twice the structure length).

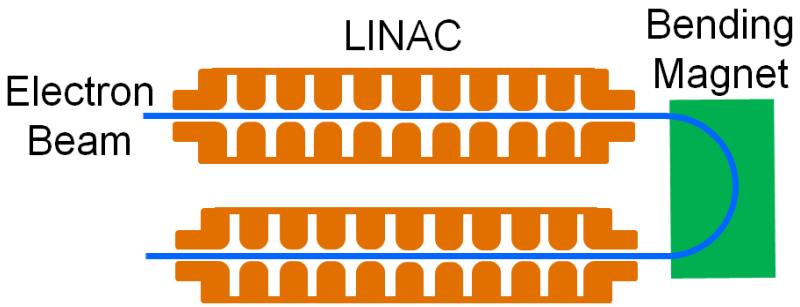

Figure 5: Schematic of a serpentine geometry accelerator with a 180° bending magnet.

See section on "Operational Temperature of Accelerator" for discussion on cryogenic temperature operation.

The power requirement estimate for generating the RF power was based on commercially available x-band amplifiers with relatively wide bandwidth. A high efficiency Class A or A/B operation amplifier with smaller bandwidth vs COST may improve efficiency.[11] Even higher efficiencies may be obtained using of Class D or F amplifiers; however operation of this amplifier type with accelerator structures has not been demonstrated to date.

Further improvements can be achieved by coupling smaller amplifier modules to individual cavities (~300 W for each cell). This distributed source design would maximize distribution efficiency and minimize weight. Using this design approach along with a narrow bandwidth SSPA, higher efficiency design class amplifiers is likely to result in a power consumption number competitive with the magnetron drive option.

Design (3): Superconducting LINAC Powered by SSPA

Advantages:

Very efficient use of RF power due to the best shunt impedance for cavities. Good for high electron beam energy and high P_b^{RF} as well.

Disadvantages:

Requires cooling to 4 K. Complex cooling can add significant weight. Operating this design with a long-term electrical power supply of less than 150 W seems unlikely and below 100 W is impossible. Mechanical robusteness of superconducting cavities (tend to be thin walled vessels) as they are deployed on a rocket of concern (unless we consider thin film deposition on bulk material).

Potential Improvements:

If the housing for the cryogenic chamber of the superconducting LINAC is at a lower temperature then less thermal power seeps into the system and needs to be dissipated. Nominally, this colder temperature of operation would be achieved by using a radiative cooler that does not draw power. However, it might be necessary to have active cooling by raising the temperature of the radiator.

Design (4): Normal-Conducting Microtron Powered by SSPA

Advantages:

Solid-state RF sources do not require a high-voltage modulator. SSPA requires power only when the microtron is on, unlike RF sources with thermionic cathodes. Very efficient use of RF power due to multiple passes of the electron beam in a single cavity. This is the most compact accelerator design (20 cm x 20 cm x 20 cm). Good for high P_b^{RF}.

Disadvantages:

Lowest level of technical readiness out of the approaches considered. Requires advanced design work to demonstrate feasibility. Longer RF duty cycles better to limit the electron beam current in the microtron.

Potential Improvements:

See section on "Operational Temperature of Accelerator" for discussion on cryogenic temperature operation.

A lower duty cycle of operation is possible if the electron beam quality produced can be maintained at higher currents. This would improve the electrical efficiency of the accelerator.

The accelerating cavity was not optimized and the shunt impedance could be improved with additional effort improving overall efficiency.

Electron Beam Source

We must also consider the requirements for the source of the electron beam which is injected into the accelerator. The power consumption of the electron source is a small fraction of the overall requirement, but it does have a noticeable impact on the performance of the overall system. In general, the higher the energy of the electrons when they are injected the better the performance of the LINAC. In practice an electron beam energy of even 10 keV is sufficient.

Pulsed DC Thermionic Electron Gun

A pulsed DC electric field can be used to accelerate electrons to an energy that is suitable for injection into the accelerator. The continuous electron beam is emitted from a thermionic cathode and accelerated by a pulsed DC electric field which is turned on and off following the RF duty cycle. It is reasonable to expect that at 10 keV 25% of the beam would be captured. With a desired average beam current over the RF duty cycle of 100 μA exiting the LINAC this requires 4 W of electrical power for the high voltage power supply (See Appendix C), which is a modest requirement compared to the power consumption of the accelerator. Approximately 25 W of CW power are required for the thermionic heater.

For accelerator designs (1), (2) and (4) we recommend this approach because it is simple and operates with low power. The power requirements are included in Table 4 for a CW injection with a DC gun for designs (1, 2 and 4).

This approach is not practical for the superconducting design (3), because the power from the electron beam which is not captured and accelerated would be deposited into the superconducting LINAC. This would overwhelm the thermal cooling power of the satellite. It is possible that a gridded cathode could be used to control emission within the time frame of one RF cycle at 1.3 GHz, but this would require additional design work to verify the improvement to the capture percentage and thermal load in the accelerator.

Normal-Conducting Thermionic RF Electron Gun

A thermionic emitter inside of a RF cavity emits a pulse of electrons during half of the RF cycle, predominantly during the portion of the cycle with the most intense electric fields. The majority of the electron bunch emitted from the electron gun is captured and accelerated by the LINAC. Even for the superconducting design (3), For the satellite based accelerator would require a normal-conducting thermionic RF gun. The RF gun cannot be superconducting because the radiative heat load from the thermionic emitter would be prohibitive for the cooling system on a satellite. We list the performance parameters for the normal-conducting RF gun for all LINAC design cases (1-3) in Table 5. Table 5 indicates that the power requirement for design case (1) and (2) are similar to a pulsed DC electron gun. However, switching to a RF gun adds a significant amount of complexity and could render it a poor trade off. For design (3) the power requirements are included in Table 4 for a normal-conducting RF gun. Additionally, approximately 25 W of CW power are required for the thermionic heater. An alternate approach to consider in a more detailed design is a superconducting RF gun with a photo or field emitter.

Table 5: Normal-Conducting RF Gun Performance

Design Case	Freq. (GHz)	D_{RF} (%)	Number of Cells	Length (m)	RF Power (W)
1	9.3	0.1	2.5	0.081	2.1
2	9.3	1	2.5	0.081	5.12
3	1.3	100	0.5	0.115	21.07

Initial Beam Emittance

The initial emittance of the electron beam will not be the same for all accelerator designs, because of the varying peak current required by the electron gun. A higher peak current will require a larger emitter which will increase the transverse emittance of the electron beam. For the thermionic emitter used in the electron gun we can estimate the thermal emittance of the electron beam to be $\varepsilon = \sigma_x \sqrt{\frac{k_B T}{mc^2}}$, where σ_x is the cathode radius.[12] We assume the thermionic emitter is a dispenser cathode operating at 1050 ^{o}C, with 5 A/cm^2 and a lifetime of ~50,000 hours.[13] Figure 6 shows the emitter size and thermal emittance as a function of duty cycle for the electron gun.

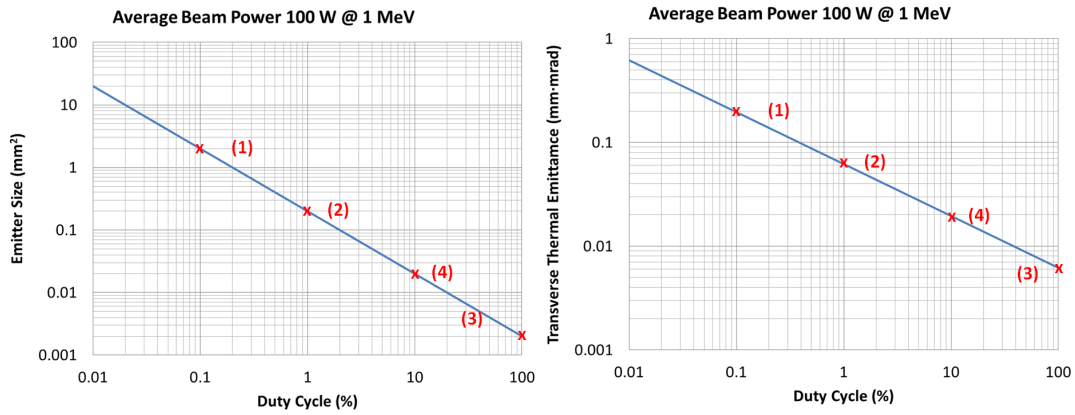

Figure 6: (left) Emitter area as a function of duty cycle. (right) Transverse emittance as a function of duty cycle.

Operational Temperature of Accelerator

For all design cases reducing the operational temperature should be favorable from a performance perspective. In the case of normal-conducting cavities the resistivity of copper can be reduced by a factor of 2 when operating at 150 K vs 300 K in the frequency range of interest.[14,15,16] This reduction in ohmic losses will double the shunt impedance and halves the RF power required to establish the accelerating gradient. Predominantly this benefits design case (2) and (4) which operate with longer duty cycles. In both cases P_b^m increases by ~10%.

Nominally, a passive radiator removes enough thermal energy to operate at 150 K. We can calculate the thermal power radiated from a black body with the equation $q=\epsilon A\sigma(T_r^4-T_s^4)$ where q is the heat dissipated, ϵ is the emissivity, A is the radiator area, σ is the Stefan-Boltzmann constant, T_r is the radiator temperature and T_s is the black body temperature of space (4 K).[17] Assuming that the long term heat load from the operation of the accelerator at 150 K is ~50 W (25 W for the thermionic heater and 25 W from RF losses) the passive radiator requires an area of 1.9 m^2. If the heat load was higher a heat exchanger could be added between accelerator and the radiator to raise the temperature and cooling power of the radiator.

An additional advantage of operating at cryogenic temperatures is that the accelerator can be placed in a cryogenic bath which is maintained at the boiling point of the cryogen. With this approach the system is more tolerant to temperature fluctuations because of excess thermal energy (which cannot be immediately handled by the thermal cooling system) results in boiling of the cryogen. However, if the accelerator remains immersed it is at the fixed temperature of the liquid. When the thermal energy is dissipated the evaporated gas condenses and returns to the liquid bath. This technique is commonly used for thermal stability of cryogenic magnets. With the low thermal average power of these accelerators it is conceivable that this negates the need for a water cooling system for the normal-conducting accelerators. Table 6 lists candidate noble gases, with Krypton and Xenon as leading candidates.

Table 6: Noble Gas Boiling Points

Noble Gas	Helium	Neon	Argon	Krypton	Xenon	Radon
Boiling Point (K)	4.4	27.3	87.4	121.5	166.6	211.5

Focusing and Steering Magnets

To control the electron beam in the LINAC and when it is ejected from the satellite we require a set of magnetic optics. These could be configured in a variety of ways, but we consider a flexible arrangement here that consists of two solenoids with one located at the injector and at the other near the end of the LINAC. Additionally, two pairs of steering magnets are also located near the start and end of the LINAC. If we consider solenoids with a focal length of 1 m, the strength of the magnetic field needed is very different because the beam energy is very different at the start and end of the LINAC. Table seven lists the specifications for the solenoids and the steering coils. It is also possible to provide focusing with permanent magnets which would not require electrical power.

Table 7: Magnetic Optics Specifications

Magnet	Integrated Field (G·cm)	Max. Power (W)	Quantity	Weight
Solenoid[18] – Injector	950	1.8	1	24
Solenoid - Exit	2500	12.3	1	24
Steering[19]	401	3.4	2	24

Space Craft Charging

Space craft charging is a legitimate concern with operating a high average power accelerator on a satellite. Without any mechanisms (*e.g.* ion gun) to neutralize the buildup of charge, previous studies by M. Franzi, shown in Figure 7, indicate that a space-plasma density of $n_e=n_i=10^4/m^3$ in the vicinity of the satellite would allow for CW operation at the P_b^m listed in Table 4 with a ~7% reduction in beam energy.

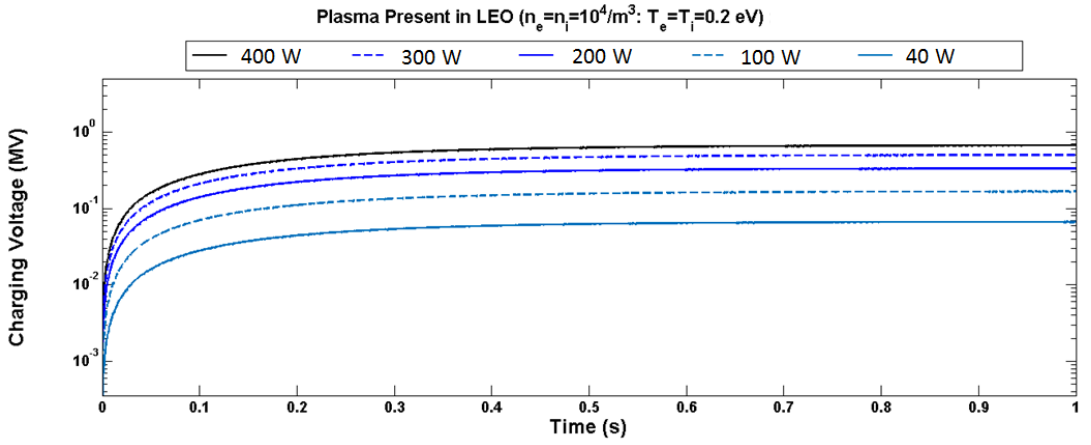

Figure 7: LEO orbit model for space craft charging.

Conclusion

We have presented a survey of accelerator technologies which can achieve the target parameters of the COMPASS proposal. We focused our efforts on four technical approaches to the accelerator: (1) normal-conducting LINAC powered by a magnetron, (2) normal-conducting LINAC powered by a SSPA, (3) superconducting LINAC powered by a SSPA and (4) normal-conducting microtron (multi-pass cavity) accelerator powered by a SSPA. The four technologies produced a similar amount of electrical beam power ($P_b{}^m$) exiting the satellite for the electron beam parameters investigated in this report. Final selection of a technology will primarily require an assessment of secondary considerations such as technical readiness; reliability; consistency of electrical power supplied by satellite; and desired range of operation for the electron beam energy, current and power.

Appendix A: RF Source Technology

a. 9.3 GHz Magnetron – Design (1)

i. CPI Magnetron VMX3045 400 kW X-band

Weight	6 kg
Peak Voltage	30 kV
Peak Current	28 A
Peak Power	400 kW
Duty Cycle	0.1%
Pulse Width	3.5 µs
Rep. Rate.	285 Hz
Average RF Power	400 W
Average Wall Power	840 W
Wall-Plug Efficiency (Excludes Heater Power)	47.6%
Heater Power	54 W
Warm-up	150 s
Total Wall-Plug Efficiency	44.24%

ii. Coaxial Pulsed Magnetron L6170 - L3 – 1.7 MW X-band

Weight	16 kg
Peak Voltage	38 kV
Peak Current	88 A
Peak Power	1.7 MW
Duty Cycle	0.08%
Pulse Width	4 µs
Rep. Rate.	200 Hz
Average RF Power	1360 W
Average Wall Power	2675 W
Wall-Plug Efficiency (Excludes Heater Power)	51%
Heater Power	150 W
Warm-up	300 s
Total Wall-Plug Efficiency	48.1%

b. 9.3 GHz SSPA – Design (2)

X-Band GaN Solid State Power Amplifier – CPI – 900 W single unit, up to 6 kW combined

Weight	4 kg
Prime Voltage	42 V
Prime Current	9.5 A
Peak Power	900 W
Duty Cycle	10 %
Average RF Power	90 W
Average Wall Power	420 W
Wall-Plug Efficiency	21.4%

c. 1.3 GHz SSPA – Design (3)

L-Band GaN Solid State Power Amplifier – CPI – 700 W single unit

Weight	32 kg
Prime Voltage	240 V
Prime Current	8 A
Peak Power	700 W
Duty Cycle	100 %
Average RF Power	700 W
Average Wall Power	1920 W
Wall-Plug Efficiency	36.4%

d. 1.3 GHz Pulsed SSPA – Design (4)

L-Band GaN Solid State Power Amplifier – CPI – 700 W single unit (Pulsed version of Appendix A.c)

Weight	6.8 kg
Prime Voltage	48 V
Prime Current	3.5 A
Peak Power	700 W
Duty Cycle	10 %
Average RF Power	70 W
Average Wall Power	168 W
Wall-Plug Efficiency	41.6%

Appendix B: High Voltage Modulators

The maximum average power needed by the magnetron is 840 W (Appendix A.a.i), but this is in excess of what is required by the LINAC. For the operation described in this report an average power of 200 W is sufficient. The modulators listed below can meet the full specifications of the magnetron, but are in excess of what is needed for the accelerator. However, the size and weight of the high voltage modulator is driven by the peak voltage and current and would roughly remain unchanged. We assume a wall-plug electrical efficiency of 61.4% for these devices for usable electron beam in short pulse (μs) operation.[20]

e. DTI – PowerMod Magnetron Modulator and Transmitter

Peak Voltage	38 kV
Peak Current	65 A
Peak Power	1 MW
Average Power	4 kW
Weight	244 kg
Size	35”x26”x21”

f. Scandinova – Magnetron Modulator M1

Peak Voltage	30-52 kV
Peak Current	30-120 A
Peak Power	1-3 MW
Average Power	2.8 kW
Weight	129 kg
Size	42 cm x 26 cm x 21 cm

B. Electron Gun Power Supply

a. Matsusada Precision - COR-10B2 series

Peak Voltage	±10 kV
Average Current	2 mA
Average Power	20 W
Min. Duty Cycle	0.2 %
Size	44 cm x 44 cm x 19 cm

References

[1] RSDO Rapid III Catalog - Spacecraft Characteristics Summary
http://rsdo.gsfc.nasa.gov/images/RSDO_Catalog_15-0401-v1.pdf

[2] Dolgashev, Valery, et al. "Status of high power tests of normal conducting single-cell standing wave structures." *Conf. Proc. C100523: THPEA060, 2010*. No. SLAC-PUB-15117. SLAC National Accelerator Laboratory (SLAC), 2012.

[3] Graves, W. S., et al. "Compact x-ray source based on burst-mode inverse Compton scattering at 100 kHz." *Physical Review Special Topics-Accelerators and Beams* 17.12 (2014): 120701.

[4] Tanabe, Eiji. "Voltage breakdown in S-band linear accelerator cavities." *Nuclear Science, IEEE Transactions on* 30.4 (1983): 3551-3553.

[5] Posen, S., M. Liepe, and D. L. Hall. "Proof-of-principle demonstration of Nb3Sn superconducting radiofrequency cavities for high Q0 applications." *Applied Physics Letters* 106.8 (2015): 082601.

[6] Halbritter, J. "Comparison between measured and calculatedRF losses in the superconducting state." *Zeitschrift für Physik* 238.5 (1970): 466-476.

[7] Cryo-coolers in Space, http://www.eng.ox.ac.uk/cryogenics/research/cryocoolers-for-space-applications

[8] Collaudin, Bernard, and Thomas Passvogel. "The FIRST and PlanckCarrier'missions. Description of the cryogenic systems." *Cryogenics* 39.2 (1999): 157-165.

[9] Bradshaw TW, Orlowska AH. Technology developments on the 4 K Cooling system for Planck and FIRST, Proc. 6th European Symposium on Space Environmental Control Systems, ESA SP-400, 1997;2:465–70

[10] Neodynium Magnets, http://www.kjmagnetics.com/products.asp?cat=1

[11] Shigematsu, H., et al. "C-band 340-W and X-band 100-W GaN power amplifiers with over 50-% PAE." *Microwave Symposium Digest, 2009. MTT'09. IEEE MTT-S International*. IEEE, 2009.

[12] http://uspas.fnal.gov/materials/10MIT/Lecture2_EmissionStatisticsCathodeEmittance_text.pdf

[13] http://www.spectramat.com/pdf/TB-105-B%20Tungsten%20Dispenser%20Cathodes%2001-13.pdf

[14] Matula, Richard Allen. "Electrical resistivity of copper, gold, palladium, and silver." *Journal of Physical and Chemical Reference Data* 8.4 (1979): 1147-1298.

[15] Rogers, J. T., et al. "Anomalous rf magnetoresistance in copper at 4 K." *Applied physics letters* 52.26 (1988): 2266-2268.

[16] Saversky, A. J., and I. S. Shchedrin. "Measurement of microwave properties of X-band accelerating structure under pulsed high-power operation at liquid nitrogen temperature." *Particle Accelerator Conference, 1993., Proceedings of the 1993*. IEEE, 1993.

[17] Jones G. Thermal analysis and testing of a spaceborne passive cooler. DPhil thesis, Clarendon Laboratory, University of Oxford, 1994.

[18] http://www.radiabeam.com/upload/catalog/pdf/136555354420130319_EMS-217-250.pdf

[19] http://www.radiabeam.com/upload/catalog/pdf/142117691820l5-01-13_STM-01-340-110.pdf

[20] Kemp, Mark, Allan Jensen, and Jeffrey Neilson. "A self-biasing pulsed depressed collector." *Electron Devices, IEEE Transactions on* 61.6 (2014): 1824-1829.